Delta-doped $SrTiO_3$ top-gated field effect transistor

Cite as: Appl. Phys. Lett. **114**, 231605 (2019); doi: 10.1063/1.5090269
Submitted: 25 January 2019 · Accepted: 28 May 2019 ·
Published Online: 13 June 2019

Hisashi **Inoue**,[1,a)] Hyeok **Yoon**,[1] Tyler A. **Merz**,[1] Adrian G. **Swartz**,[1] Seung Sae **Hong**,[1] Yasuyuki **Hikita**,[2] and Harold Y. **Hwang**[1,2]

AFFILIATIONS

[1]Geballe Laboratory for Advanced Materials, Department of Applied Physics, Stanford University, Stanford, California 94305, USA
[2]Stanford Institute for Materials and Energy Sciences, SLAC National Accelerator Laboratory, Menlo Park, California 94025, USA

[a)]**Present address:** Frontier Research Institute for Interdisciplinary Sciences and Institute for Materials Research, Tohoku University, Sendai 980-8577, Japan. **Electronic mail:** hisashi.inoue@fris.tohoku.ac.jp

ABSTRACT

Oxide heterostructures are an attractive platform for incorporation in field-effect transistors (FETs) due to their diverse physical properties which can be tuned by electrostatic gating. We report a top-gated FET based on a $SrTiO_3$ delta-doped structure, which operates down to cryogenic temperatures. The device shows excellent DC characteristics with an on/off ratio greater than 10^4 and field effect mobility estimated to be 2125 $cm^2/V\,s$ at 2 K. The high field effect mobility was consistent with the Hall mobility and is attributed to the formation of a two-dimensional electron system in the delta-doped layer: two-dimensional gate-tunable Shubnikov-de Haas oscillations confirm this. The achievement of an electron density of $3 \times 10^{12}\,cm^{-2}$ in a gate-tunable geometry allows for the exploration of the interplay between magnetic, ferroelectric, and superconducting properties of $SrTiO_3$ in the quantum limit.

Two-dimensional electron systems (2DES) formed in $SrTiO_3$-based heterostructures have been actively studied owing to their unique characteristics such as the coexistence of high-mobility electrons,[1–3] superconductivity,[4] and magnetism.[5–7] Among various systems studied, the $SrTiO_3$ delta-doped structure is a highly flexible platform to study the 2DES with adjustable carrier density and electron confinement over a wide range. Recent reports on this system include the quantum Hall effect in the low density limit[3] and the coexistence of 2D superconductivity and 2D high mobility electrons in the higher density regime.[8,9] On the other hand, the application of an electric field via top-gating is a precise way to tune electronic properties as demonstrated in many other $SrTiO_3$ 2DES owing to its low carrier density and large dielectric constant.[10–25] Therefore, combining the top-gating technique with the $SrTiO_3$ delta-doped structure will enable precise control over physical parameters in a wide range, thus allowing for exploration of the interplay of a variety of physical phenomena in $SrTiO_3$.

In this letter, we report a top-gating device using a $SrTiO_3$ delta-doped channel. The delta-doped structure consists of a thin semiconducting Nb-doped $SrTiO_3$ (Nb:$SrTiO_3$) delta-doped layer, sandwiched by thick undoped $SrTiO_3$ cap and buffer layers. The confinement of the conducting channel in the delta-doped structure is defined by the Coulomb potential from the positively charged niobium dopants rather than the conduction band offset as seen at heterointerfaces. This leads to minimal interface or surface scattering, enabling high mobility.[26] To make a transistor device, we used a Au top-gate contact, which creates a Schottky junction to the delta-doped structure. As this depletes the carriers from the delta-doped layer, our transistor acts in part like a metal-semiconductor field-effect transistor (MESFET). By optimizing the confinement profile and the top-gating device geometry, the fabricated delta-doped $SrTiO_3$ FET operates at both room and low temperatures with a large on/off ratio greater than 10^4. The FET shows an estimated field effect mobility of 2125 $cm^2/V\,s$ as confirmed by the observation of 2D Shubnikov-de Haas oscillations upon gating. The very high gating sensitivity of this FET compared to previously reported back-gated devices leads to a platform on which to study the rich physical properties of $SrTiO_3$-based heterostructures through precise control of carrier density and mobility.

The delta-doped structure was epitaxially grown on a single crystal $SrTiO_3$ (100) substrate by pulsed laser deposition (PLD). The device structure and optical image are shown in Figs. 1(a) and 1(b), respectively. We used a Hall bar structure for the conducting layer of the transistor. This allows us to measure independently the Hall effect and the resistance in the four-probe geometry. The channel length and

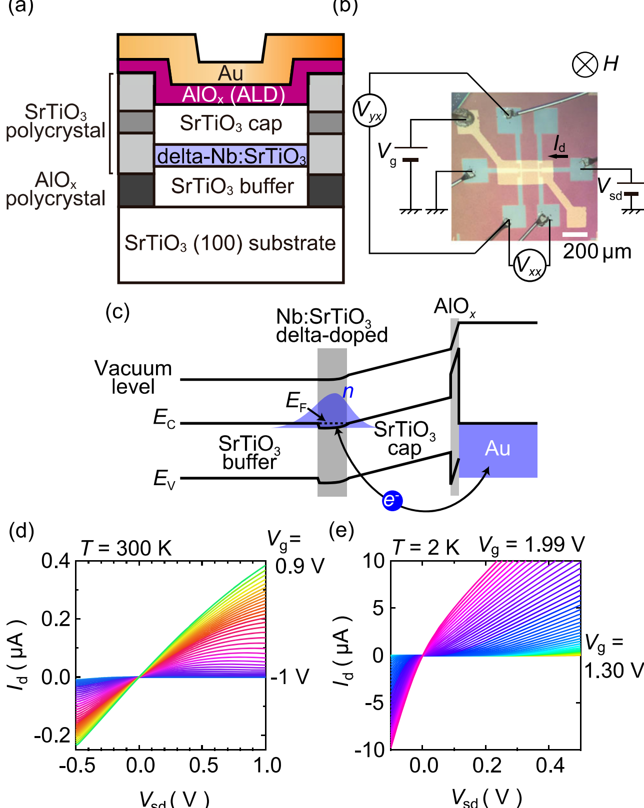

FIG. 1. (a) Device structure of the delta-doped $SrTiO_3$ FET and (b) optical image. The measurement configuration and magnetic field orientation are also shown. The source, gate, and drain electrodes are located on the left, in the middle, and on the right of the Hall bar, respectively. (c) Schematic band diagram of the delta-doped $SrTiO_3$ FET. E_C, E_V, and E_F are the conduction band energy, the valence band energy, and the Fermi energy, respectively. Drain current I_d as a function of source-drain voltage V_{sd} measured (d) at 300 K and (e) at 2 K at various gate voltages V_g in steps of 0.05 V and 0.01 V, respectively. V_{xx}, V_{yx}, and H are longitudinal voltage, transverse voltage, and magnetic field, respectively.

width of the Hall bar are 160 μm and 20 μm, respectively. Prior to the deposition of the $SrTiO_3$ and Nb:$SrTiO_3$ layers, an on-chip hard mask consisting of amorphous AlO_x was deposited to define the Hall bar using standard photolithography and electron-beam evaporation. The AlO_x-patterned $SrTiO_3$ (100) substrate was then annealed at 900 °C in the PLD chamber with an oxygen pressure of $\sim 1 \times 10^{-5}$ Torr for 50 min to remove any residual contaminants. In order to fabricate a high mobility delta-doped transistor device, we employed the growth condition reported in Ref. 27, which enables the synthesis of stoichiometric films with bulk single-crystal quality. The $SrTiO_3$ buffer (100 nm), the 0.2 at. % Nb:$SrTiO_3$ delta-doped layer (20 nm), and the $SrTiO_3$ cap (100 nm) layers were sequentially deposited at 1080 °C. After the deposition, the delta-doped structure was postannealed at 900 °C with an oxygen pressure of 1×10^{-2} Torr for 30 min to backfill oxygen vacancies. After the deposition of the delta-doped structure, the sample surface was coated with a 5 nm-thick AlO_x gate dielectric using atomic layer deposition (ALD) at 150 °C for 50 cycles using trimethylaluminum as the precursor. Subsequently, an Au top-gate electrode was deposited by electron-beam evaporation through a metal shadow mask above the channel region. The transistors were characterized in a helium cryostat at temperatures from 2 K to 300 K using a semiconductor parameter analyzer and lock-in amplifiers.

The fabricated device shows excellent FET operation both at $T = 300$ K and at $T = 2$ K. Note that the Au gate acts like a Schottky contact with respect to Nb:$SrTiO_3$, which makes the Au/AlO_x/(delta-doped $SrTiO_3$) effectively a Schottky junction as shown in Fig. 1(c). When the Schottky junction is formed, electrons are transferred from the delta-doped layer to Au to compensate the band offset, partly depleting the channel at room temperature, and completely at $T = 2$ K because of the temperature dependence of the dielectric constant of $SrTiO_3$, which significantly increases at low temperatures. The drain current (I_d) systematically increases with both the source-drain voltage (V_{sd}) and gate voltage (V_g) as shown in Figs. 1(d) and 1(e) for $T = 300$ K and $T = 2$ K, respectively. By reducing the gate voltage, the drain current can be turned off with an on/off ratio exceeding 10^4 at both temperatures and with minimal gate leakage I_g less than 20 pA ($T = 300$ K) and 700 pA ($T = 2$ K), respectively [see Figs. 2(a) and 2(b)]. I_g was measured between the gate electrode and the source electrode in Fig. 1(b). The sign of I_g changes from negative to positive when V_g is increased across the threshold voltage, as was observed in previous field effect transistor devices.[17,28] The larger I_g at 2 K is possibly due to the larger electron concentration in the $SrTiO_3$ cap region than at 300 K as discussed below.

Figures 2(a) and 2(b) show a line cut of the data in Figs. 1(d) and 1(e) at fixed V_{sd}, respectively. I_d increases monotonically as V_g increases at both $T = 300$ K and 2 K. The on/off ratio of greater than 10^4 is demonstrated in the log-scale plots in Figs. 2(c) and 2(d). The absolute value of I_d is enhanced ~20 times at 2 K than at 300 K. The

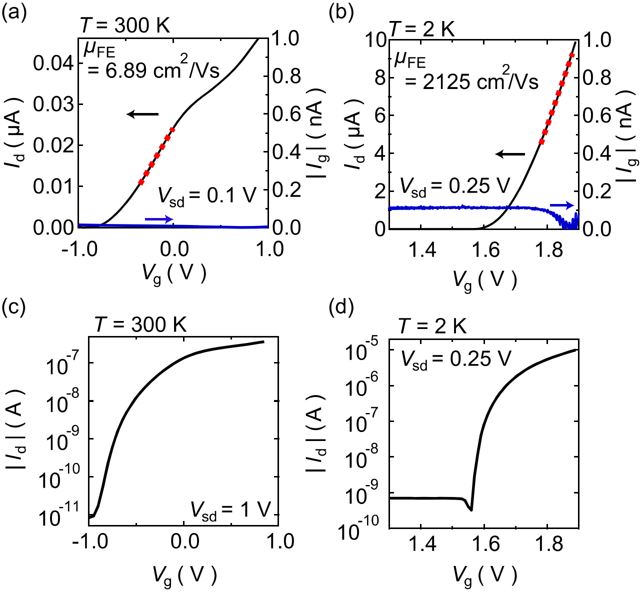

FIG. 2. V_g dependence of I_d (left axis) and absolute value of the gate leakage $|I_g|$ (right axis) measured at (a) 300 K and (b) 2 K. Linear fits to the linear region of $I_d(V_g)$ are shown as dashed lines. Absolute values of I_d shown on a log scale demonstrating an on/off ratio $>10^4$ (c) at 300 K and (d) at 2 K.

slope dI_d/dV_g reflects the field effect mobility in the electron drift regime. To estimate the field effect mobility, we assumed a simple parallel capacitor model and a delta-function like distribution of the electrons centered at the middle of the delta-doped layer. We used the dielectric constants of $SrTiO_3$ $\varepsilon_{STO} = 277\varepsilon_0$ and $26\,000\varepsilon_0$ for $T = 300$ K and $T = 2$ K, respectively,[29,30] and the dielectric constant of AlO_x $\varepsilon_{AlOx} = 9\varepsilon_0$, where ε_0 is the vacuum permittivity. This approach neglects a proper treatment of the finite spread of electrons beyond the delta-doped layer. In order to evaluate the error introduced by this simplification, we calculated n_s as a function of V_g using self-consistent model calculations (extending Ref. 8) and compared it with the parallel capacitor model. We found that the error for the gate capacitance $\propto dn_s/dV_g$ due to the spread of electrons is <4% at $T = 300$ K and <0.2% at $T = 2$ K, where n_s is the sheet electron density in the channel. The reason for this close correspondence is the much lower dielectric constant of AlO_x compared to $SrTiO_3$; the gate capacitance is dominated by the capacitance across AlO_x and is relatively insensitive to changes in the effective thickness of the $SrTiO_3$ cap layer. Thus, the linear fits shown in Fig. 2(b) yield the field effect mobility $\mu_{FE} = 2125\,cm^2/V\,s$ at 2 K, dramatically increased from $\mu_{FE} = 6.89\,cm^2/V\,s$ at $T = 300$ K [Fig. 2(a)]. This low temperature field effect mobility is comparable to the initial report in GaAs delta-doped FET at 77 K[31] despite the heavier effective mass in $SrTiO_3$. This exceeds the mobility reported for the delta-doped FET using $CaHfO_3$[32] and is comparable to the values reported for many solid dielectric top-gated $SrTiO_3$-based FETs that operate in this carrier density range.[12,17,33,34]

The magnetoresistance (MR) and Hall effect measured at $T = 2$ K on the same device are shown in Figs. 3(a) and 3(b). The longitudinal resistance and Hall slope decrease with increasing V_g, indicating that electron density increases with V_g, consistent with the carrier accumulation in the delta-doped channel. We observe a nonlinear Hall effect and analyze the Hall curves using a two-carrier model[35] [Fig. 3(c)]. It shows an excellent fit to experimental data and gives the carrier density and mobility for two components n_{s1}, n_{s2} and μ_1, μ_2 shown in Figs. 3(d) and 3(e), respectively. The total carrier density $n_{total} = n_{s1} + n_{s2}$ and the average Hall mobility defined by $\mu_{ave} = (n_{s1}\mu_1 + n_{s2}\mu_2)/n_{total}$ are also plotted in the same graph. The maximum Hall mobility of $1343\,cm^2/V\,s$ corresponds well to the field effect mobility estimated above. We also note that n_{total} is linearly proportional to V_g as one would expect from a simple parallel capacitor model for the gating operation. However, the linear fit of n_{total} to V_g gives the gate capacitance $C_g = 0.87 \pm 0.02\,\mu F/cm^2$, smaller than the geometrical capacitance $C_{geom} = 1.6\,\mu F/cm^2$ estimated using the nominal thickness and the dielectric constants mentioned above. The 54% reduction of C_g may stem in part from quantum capacitance, which has been observed in low-dimensional low-density semiconductors due to shift of internal chemical potential by gate voltage.[36,37]

In order to estimate the electron confinement length around the delta-doped layer, we performed self-consistent model calculations of the band structure assuming a Thomas-Fermi distribution of electrons and using Poisson's equation. We used an average band effective mass of $1.79m_0$, where m_0 is the electron mass. Under flat-band conditions [see Figs. 4(a) and 4(b), dashed curves], electrons are confined symmetrically around the delta-doped layer, distributed over the spatial region of ~12 nm and ~52 nm at 300 K and 2 K, respectively. The wider distribution of electrons at $T = 2$ K reflects the increased

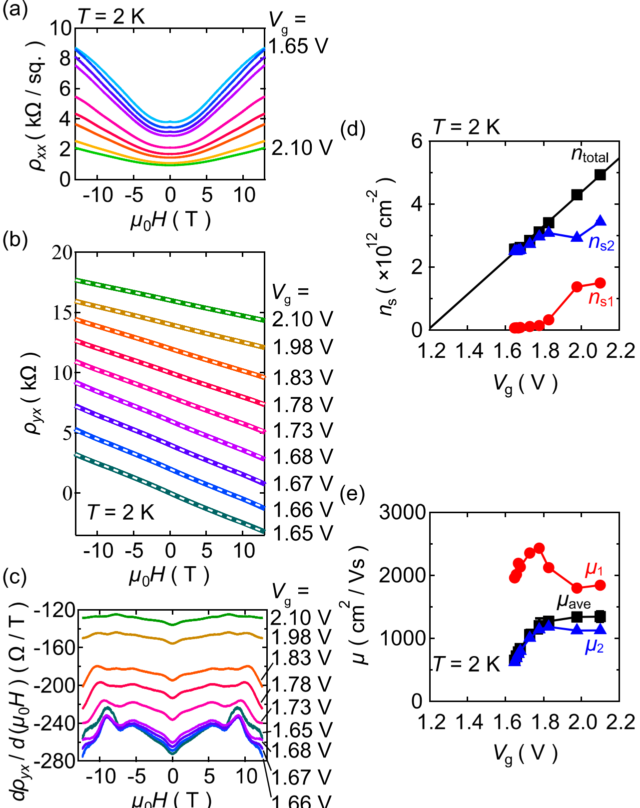

FIG. 3. (a) Longitudinal magnetoresistance $\rho_{xx}(H)$ and (b) Hall resistance $\rho_{yx}(H)$ at various V_g. Dashed curves in (b) are fit results to the two-carrier model. Vertical offsets are added for clarity in (b). (c) The differential $d\rho_{yx}/d(\mu_0 H)$ values are field dependent due to the nonlinear Hall effect and the onset of quantum oscillations. (d) and (e) Sheet carrier densities n_{s1} and n_{s2} and Hall mobilities μ_1 and μ_2 extracted from the fitting results to the two-carrier model. $n_{total} = n_{s1} + n_{s2}$ and $\mu_{ave} = (n_{s1}\mu_1 + n_{s2}\mu_2)/n_{total}$.

dielectric constant. The electron density at the center of the delta-doped channel was $3 \times 10^{19}\,cm^{-3}$ ($8 \times 10^{18}\,cm^{-3}$) at 300 K (2 K), much higher than the value at the interface between the $SrTiO_3$ cap and the AlO_x layer of $1 \times 10^{15}\,cm^{-3}$ ($6 \times 10^{17}\,cm^{-3}$), demonstrating the effective spatial separation of mobile electrons from the surface/interface, contributing to the high mobility of our FET device. In Figs. 4(a) and 4(b), solid curves show the calculated band profiles with an external gate voltage at which the sheet electron densities were 8% of the activated dopant density, corresponding approximately to $V_g = 2.1$ V. The externally applied electric field increases the slope of the conduction band energy $E_C(z)$ and makes the distribution of electrons asymmetric. For a given electron density, we see that the induced electric field is smaller by a factor of 94 at 2 K than at 300 K. This indicates that a small voltage modulation can induce more abrupt change in the carrier density and thus I_d at $T = 2$ K than at $T = 300$ K, consistent with the observation in the experiment [see Figs. 2(a) and 2(b)].

When electrons are confined in a 2D region as shown in Figs. 4(a) and 4(b), the three-dimensional Fermi surface of $SrTiO_3$ is transformed into a 2D Fermi surface. As a result, one expects 2D quantum oscillations when the mobility of electrons meets the condition

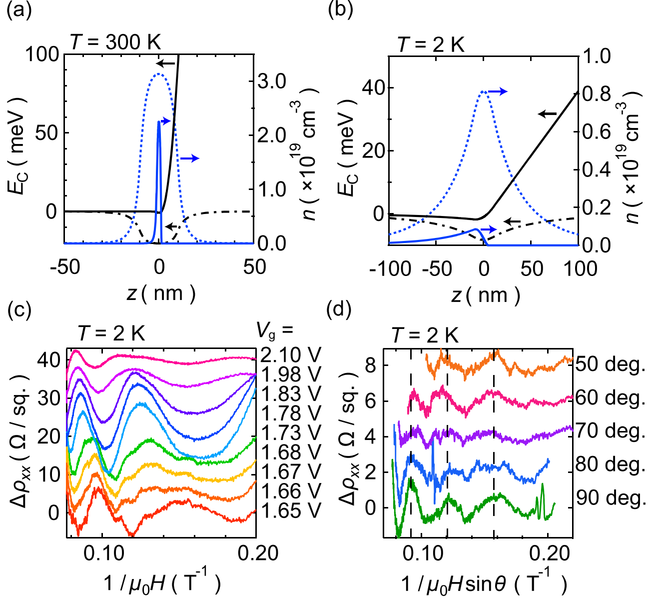

FIG. 4. (a) and (b) The calculated spatial profile of the conduction band bottom energy E_C (left axis) and electron density n (right axis) around the Nb:$SrTiO_3$ delta-doped layer. The center of the delta-doped layer is located at depth $z = 0$. Temperatures are (a) 300 K and (b) 2 K. Dashed curves correspond to the flat band condition without the Schottky contact. Solid curves are the profiles with an applied gate voltage for which the sheet electron density is 8% of the Nb dopant density. (c) Shubnikov-de Haas oscillations at various V_g extracted from Fig. 3(a) by subtracting smoothly varying backgrounds. Vertical offsets are added for clarity. (d) Angle dependence of Shubnikov-de Haas oscillations at $V_g = 2.20$ V. The horizontal axis is scaled by the perpendicular component of magnetic field $H \sin\theta$. Offsets are added for clarity. Measurement temperatures are 2 K for both (c) and (d).

$\omega_c\tau > 1$, where ω_c is the cyclotron frequency and $\tau \propto \mu$ is the scattering time. Indeed, the mobility of the electrons in the FET was high enough for the system to exhibit Shubnikov-de Haas oscillations at $T = 2$ K as shown in Fig. 4(c). The frequency of the oscillations increases monotonically as a function of V_g, indicating an expansion in the cross-sectional area of the electron pocket in k-space, which is consistent with the carrier accumulation in the delta-doped layer. We have also evaluated the evolution of SdH oscillations as a function of the magnetic field direction with respect to the sample normal. Notably, in Fig. 4(d), the phase of the oscillation is scaled by the perpendicular component of magnetic field $H \sin\theta$, where θ is the angle between the sample plane and the magnetic field, indicating that the delta-doped channel hosts a two-dimensional quantum well.

By combining DC FET characterization and Hall measurements, we have shown operation of the high mobility delta-doped $SrTiO_3$ field effect transistor both at $T = 300$ K and at 2 K. We have also shown that the delta-doped method enables access to the low-dimensional system in high mobility and low carrier density regimes by suppressing the scattering from the interface/surface. The carrier density in our FET is significantly smaller, $n_{total} \sim 3 \times 10^{12}$ cm^{-2}, than that in other $SrTiO_3$ based quantum wells, approaching the quantum limit.[2,3,38] Together with prior work on substrate-gated delta-doped $SrTiO_3$,[3] this work opens pathways to manipulate the quantum states of low-dimensional electrons in $SrTiO_3$ to explore phenomena including the quantum Hall effect[2,3] and low-dimensional superconductivity at low temperatures,[4,6,39] where the symmetry of the 2DES can be fully gate controlled.[34]

This work was supported by the Department of Energy, Office of Basic Energy Sciences, Division of Materials Sciences and Engineering, under Contract No. DE-AC02-76SF00515. T.A.M. acknowledges partial support by a NSF Graduate Research Fellowship under Grant No. DGE-114747. A.G.S. and S.S.H. acknowledge partial support by the Gordon and Betty Moore Foundation's EPiQS Initiative through Grant No. GBMF4415.

REFERENCES

[1]A. Ohtomo and H. Y. Hwang, Nature **427**, 423 (2004).
[2]Y. Xie, C. Bell, M. Kim, H. Inoue, Y. Hikita, and H. Y. Hwang, Solid State Commun. **197**, 25 (2014).
[3]Y. Matsubara, K. S. Takahashi, M. S. Bahramy, Y. Kozuka, D. Maryenko, J. Falson, A. Tsukazaki, Y. Tokura, and M. Kawasaki, Nat. Commun. **7**, 11631 (2016).
[4]N. Reyren, S. Thiel, A. D. Caviglia, L. F. Kourkoutis, G. Hammerl, C. Richter, C. W. Schneider, T. Kopp, A.-S. Rüetschi, D. Jaccard, M. Gabay, D. A. Muller, J.-M. Triscone, and J. Mannhart, Science **317**, 1196 (2007).
[5]A. Brinkman, M. Huijben, M. van Zalk, J. Huijben, U. Zeitler, J. C. Maan, W. G. van der Wiel, G. Rijnders, D. H. A. Blank, and H. Hilgenkamp, Nat. Mater. **6**, 493 (2007).
[6]J. A. Bert, B. Kalisky, C. Bell, M. Kim, Y. Hikita, H. Y. Hwang, and K. A. Moler, Nat. Phys. **7**, 767 (2011).
[7]L. Li, C. Richter, J. Mannhart, and R. C. Ashoori, Nat. Phys. **7**, 762 (2011).
[8]Y. Kozuka, M. Kim, C. Bell, B. G. Kim, Y. Hikita, and H. Y. Hwang, Nature **462**, 487 (2009).
[9]M. Kim, C. Bell, Y. Kozuka, M. Kurita, Y. Hikita, and H. Y. Hwang, Phys. Rev. Lett. **107**, 106801 (2011).
[10]K. Ueno, I. H. Inoue, H. Akoh, M. Kawasaki, Y. Tokura, and H. Takagi, Appl. Phys. Lett. **83**, 1755 (2003).
[11]K. Shibuya, T. Ohnishi, M. Lippmaa, M. Kawasaki, and H. Koinuma, Appl. Phys. Lett. **85**, 425 (2004).
[12]H. Nakamura, H. Takagi, I. H. Inoue, Y. Takahashi, T. Hasegawa, and Y. Tokura, Appl. Phys. Lett. **89**, 133504 (2006).
[13]A. D. Caviglia, S. Gariglio, N. Reyren, D. Jaccard, T. Schneider, M. Gabay, S. Thiel, G. Hammerl, J. Mannhart, and J.-M. Triscone, Nature **456**, 624 (2008).
[14]B. Förg, C. Richter, and J. Mannhart, Appl. Phys. Lett. **100**, 053506 (2012).
[15]P. Irvin, M. Huang, F. J. Wong, T. D. Sanders, Y. Suzuki, and J. Levy, Appl. Phys. Lett. **102**, 103113 (2013).
[16]M. Boucherit, O. F. Shoron, T. A. Cain, C. A. Jackson, S. Stemmer, and S. Rajan, Appl. Phys. Lett. **102**, 242909 (2013).
[17]M. Hosoda, Y. Hikita, H. Y. Hwang, and C. Bell, Appl. Phys. Lett. **103**, 103507 (2013).
[18]P. D. Eerkes, W. G. van der Wiel, and H. Hilgenkamp, Appl. Phys. Lett. **103**, 201603 (2013).
[19]A. Verma, S. Raghavan, S. Stemmer, and D. Jena, Appl. Phys. Lett. **105**, 113512 (2014).
[20]P. Gallagher, M. Lee, T. A. Petach, S. W. Stanwyck, J. R. Williams, K. Watanabe, T. Taniguchi, and D. Goldhaber-Gordon, Nat. Commun. **6**, 6437 (2015).
[21]S. Goswami, E. Mulazimoglu, L. M. K. Vandersypen, and A. D. Caviglia, Nano Lett. **15**, 2627 (2015).
[22]W. Liu, S. Gariglio, A. Fête, D. Li, M. Boselli, D. Stornaiuolo, and J.-M. Triscone, APL Mater. **3**, 062805 (2015).
[23]S. Hurand, A. Jouan, C. Feuillet-Palma, G. Singh, J. Biscaras, E. Lesne, N. Reyren, A. Barthélémy, M. Bibes, J. E. Villegas, C. Ulysse, X. Lafosse, M. Pannetier-Lecoeur, S. Caprara, M. Grilli, J. Lesueur, and N. Bergeal, Sci. Rep. **5**, 12751 (2015).
[24]C. Woltmann, T. Harada, H. Boschker, V. Srot, P. A. van Aken, H. Klauk, and J. Mannhart, Phys. Rev. Appl. **4**, 064003 (2015).

[25]S. Zeng, W. Lü, Z. Huang, Z. Liu, K. Han, K. Gopinadhan, C. Li, R. Guo, W. Zhou, H. H. Ma, L. Jian, T. Venkatesan, and Ariando, ACS Nano **10**, 4532 (2016).
[26]Y. Kozuka, M. Kim, H. Ohta, Y. Hikita, C. Bell, and H. Y. Hwang, Appl. Phys. Lett. **97**, 222115 (2010).
[27]Y. Kozuka, Y. Hikita, C. Bell, and H. Y. Hwang, Appl. Phys. Lett. **97**, 012107 (2010).
[28]G. Singh-Bhalla, C. Bell, J. Ravichandran, W. Siemons, Y. Hikita, S. Salahuddin, A. F. Hebard, H. Y. Hwang, and R. Ramesh, Nat. Phys. **7**, 80 (2011).
[29]T. Sakudo and H. Unoki, Phys. Rev. Lett. **26**, 851 (1971).
[30]K. A. Müller and H. Burkard, Phys. Rev. B **19**, 3593 (1979).
[31]E. Schubert, A. Fischer, and K. Ploog, IEEE Trans. Electron Devices **33**, 625 (1986).
[32]K. Nishio, M. Matvejeff, R. Takahashi, M. Lippmaa, M. Sumiya, H. Yoshikawa, K. Kobayashi, and Y. Yamashita, Appl. Phys. Lett. **98**, 242113 (2011).
[33]H. Nakamura, T. Koga, and T. Kimura, Phys. Rev. Lett. **108**, 206601 (2012).
[34]Z. Chen, A. G. Swartz, H. Yoon, H. Inoue, T. A. Merz, D. Lu, Y. Xie, H. Yuan, Y. Hikita, S. Raghu, and H. Y. Hwang, Nat. Commun. **9**, 4008 (2018).
[35]N. W. Ashcroft and N. D. Mermin, *Solid State Physics* (W.B. Saunders, Philadelphia, PA, USA, 1976).
[36]S. Luryi, Appl. Phys. Lett. **52**, 501 (1988).
[37]L. Li, C. Richter, S. Paetel, T. Kopp, J. Mannhart, and R. C. Ashoori, Science **332**, 825 (2011).
[38]Y. Kozuka, T. Susaki, and H. Y. Hwang, Phys. Rev. Lett. **101**, 096601 (2008).
[39]G. Cheng, M. Tomczyk, S. Lu, J. P. Veazey, M. Huang, P. Irvin, S. Ryu, H. Lee, C.-B. Eom, C. S. Hellberg, and J. Levy, Nature **521**, 196 (2015).